RT&A, No 4(80)
Volume 19, December, 2024

EXPERIMENTAL AND NUMERICAL INVESTIGATION OF STRESS CONCENTRATION FACTOR FOR POLYGONAL DISCONTINUITIES IN A FINITE PLATE

Rashmiben H. Patel[1,2], Dr. Bhaveshkumar P. Patel[3]

•

1 Ph. D Scholar, Faculty of Engineering and Technology, Ganpat University, Ganpat Vidhyanagar 384012, Mehsana, Gujarat, India. rashmibeme@gmail.com

2 Assistant Professor, Department of Mechanical Engineering, Government Engineering College, Gandhinagar, 382028, Gujarat, India. rashmimech@gecg28.ac.in

3 Professor, Department of Mechanical Engineering, U. V. Patel College of Engineering, Ganpat University, Ganpat Vidhyanagar - 384012, Mehsana, Gujarat, India, bpp01@ganpatuniversity.ac.in

Corresponding Author E-mail. (bpp01@ganpatuniversity.ac.in)

Abstract

Structural steel is widely utilized in the construction engineering sector to build a variety of buildings, including flyovers, skyscrapers, plants, heavy machinery vehicle structures, etc., in different combinations. Due to their wide range of applications, particularly in the automotive and aerospace industries, plates with different kinds of holes are also significant parameters for mechanical design. To satisfy the requirements in the final structure design, these holes are formed into plates. However, these holes concentrate stress, which gradually weakens the structure's mechanical strength. The present study aims to reduce this stress concentration of compressed plates having polygonal holes of varying shapes and sizes. The stress concentration factor around polygonal holes in polycarbonate plates, subject to uniaxial compression loads, is investigated experimentally and numerically. To obtain solutions, three approach are adopted; the finite element method, DOE RSM (Response Surface Methodology) and photoelasticity are used as the experimental method. The study's conclusions are presented here in the form of numerical and graphical data, along with a comparison between the outcomes and the photo-elasticity test results.

Keywords: Finite element method, finite plate, structural discontinuity, polygonal holes, photoelasticity, stress concentration factors

Abbreviation:

RSM	Response Surface Methodology
FEA	Finite Element Analysis
DOE	Design of Experiment
SCF	Stress Concentration Factor
FGM	Finite Graded Material
FEM	Finite Element Method
CNC	Computerized Numerical Control

Notations:

N	Fringe number
f_σ	Stress fringe value (stress fringe constant of model material)
t	Thickness of the plate (mm)
K_t	Stress concentration factor
H	Height of plate (mm)
L	Length of plate (mm)
l	Side of polygonal hole (mm)
l/L	Side ratio
n	Number of side of polygonal hole in a plate
O	Polygonal hole orientation (°)
A	Area of the polygonal hole (mm^2)
P	Applied load (N)
σ_{max}	Maximum stress at the discontinuity (N/mm^2)
σ_{nom}	Nominal or background stress (N/mm^2)
d	Maximum length of polygonal hole along the loading direction (mm)

1. Introduction

Optimization of the structure's shape has been prompted by the growing demand for lightweight, energy-efficient structures in recent years. Structural elements must have various cut-out shapes lighten the system's weight and allow access to other structural components. It is commonly known that highly localized stresses are created in the area around a cut-out or hole in a stressed member. Geometric irregularities like different shoulder fillets, grooves (U, V, Square), keyways, threads, notches, holes, etc., found on plates are essential features because they fulfill specific operational needs. These geometric discontinuities will generate stress concentrations. To design a component or a structure, it is necessary and helpful to estimate the stresses and strains at these geometries. Due to the application of this discontinuities in marine and aerospace structures, thin plates are frequently used. Different kinds of holes or openings are usually made in the plates for practical reasons, like reducing the weight of the system and providing access to its components. When a plate undergoes tension, compression, or shear forces, the presence of holes or openings results in increased stresses in their vicinity. For the best design and resistance to mechanical failure, understanding of the stress distribution surrounding the hole is essential. An experimental methodology can be employed to determine the maximum stress concentration for various complex geometries while taking into account time or cost limitations. The number of sides, orientations of polygonal hole, areas of the polygonal hole, and applied load on a finite plate are four variable parameters considered in the calculation.

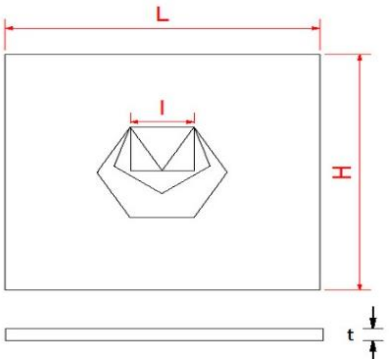

Figure 1: *The geometry of polygonal hole in a plate*

Figure 1 shows flat plate with polygonal hole. A stress concentration is defined as the ratio of the maximum stress within the element to the nominal stress (reference stress).

$$K_t = \frac{\sigma_{max}}{\sigma_{nom}} \quad (1)$$

$$\sigma_{nom} = \frac{P}{(H-\mathrm{d}) \times t} \quad (2)$$

Numerous researchers consistently focus on the stress concentration problem associated with a plate containing a hole, which is a crucial consideration in structural design.

An analysis of stresses and strains in finite and infinite rectangular homogeneous, isotropic elastic plates with a circular hole was provided by M. Ismail et al. under uniform tensile loading [1]. M. Pandey conducted an examination of stress distribution within a plate featuring an inclined circular aperture under varying uniaxial tensile loads. Utilizing finite element analysis (FEA) in ANSYS, stresses were determined for circular holes inclined at angles of 30°, 45°, and 90°. The investigation revealed that the minimum stress concentration factor occurred at a 45° inclination angle, while the maximum SCF was observed for a vertically oriented hole, inclined at 90° [2]. Xiaoli Zhang al. studied the stress generation in infinite skew anisotropic infinite plate with elliptical hexagonal and square holes with the use of the analytical method [3]. A novel analytical-numerical technique is introduced for assessing the combined stresses induced by multiple circular apertures within an infinite elastic plate. This method accounts for both externally applied remote stresses and arbitrarily distributed stresses along the circular boundaries. This method is based on elementary solutions and new integral equations [4]. The elastic stress around a various holes (circle, an ellipse, and overlapping circles) with corners in an infinite plate subjected to biaxial stress was observed by W. Wang et al. Complex Goursat functions are used to formulate the elasticity problem, leading to a set of singular integro-differential equations on the boundary [5]. The distribution of stress in an infinite plate experiencing uniaxial tension with an ellipse or circular hole was calculated using the boundary force method [6]. B. Safaei et al. compared the numerical results with analytical answers after investigating the stress distribution in sheets with circular cutouts and studying stress concentration at the edge of holes [7]. Jaiswal et al. employed a technique to model functionally graded material (FGM) within the finite element method (FEM)-based software ANSYS. They aimed to mitigate stress concentration by implementing an FGM ring around the rounded rectangular slot under tensile loading [8]. Rani et al. further expanded their research by utilizing the extended finite element method to quantitatively analyze the stress concentration around a centrally positioned elliptical inclusion embedded within functionally graded material [9].

Using integral equations based on Green-type solutions, O. Maksymovych et al. determined the impact of stress concentration near cracks, holes, and dies, in the dynamic loading and half plane plate. [10] [11]. M. Patil et al. determined the influence of roundness and orientation of hexagonal cutouts on stress concentration in a plate subjected to tensile loading [12]. M. M. Kumar et al. conducted a study investigating the impact of cut-out orientation and bluntness in an aluminum plate featuring triangular and square cut-outs under uniaxial loading conditions. [13]. The effect of side ratio and height ratio on SCF of polygonal cutout in a finite plate was discussed by R. Patel et al. [14].

The additional auxiliary hole arrangements, different reinforcing thicknesses, hole position, shape, and size, as well as the ratio of the various polygonal holes to the plate size, are all impacted by the stresses that are created in a plate. It demonstrates that the most important design component is the length and that varying the location of the holes can reduce stress concentration [15].

2. Methods

In recent years, the use of computer methods for structural optimization using Finite element analysis (FEA) has grown significantly in the research and development process. The computational cost of these optimization procedures varies according to the problem's complexity. Utilizing DOE (RSM) techniques in conjunction with FEA results in a significant reduction in computing effort without compromising research outcomes.

2.1 Finite Element Analysis

Finite element analysis (FEA) was employed to analyze computational results for different parameters of various flat plate geometries. For all the four parameters (the number of sides, orientations of polygonal hole, areas of the polygonal hole, and applied load on a finite plate) for polygonal hole shapes in a finite flat plate are modelled and analyzed. ANSYS workbench 20 R1 is used for the FEA of all the geometries. Special polygonal-shaped holes are incorporated into a plate to fulfill specific structural requirements, typically using structural steel such as IS 2062, which is commonly utilized across industries. In this study, the plate material conforms to the IS 2062 standard, reflecting prevalent industrial practices. The American equivalent standard is ASME SA 36/ASTM A36 steel.

Figure 2 represent the 2D and 3D model for the plate with hole of various geometric shapes like triangular, square, pentagonal, and hexagonal. The units for geometrical dimensions and force are millimeter and Newton respectively.

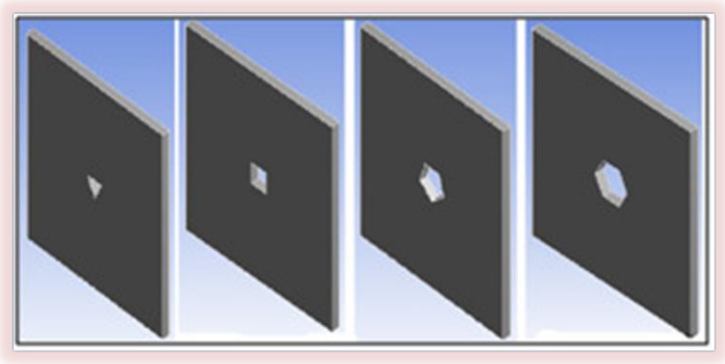

(a) Triangular, (b) square, (c) pentagonal, (d) hexagonal holes
Figure 2: *3D model of plate with polygonal hole*

The finite element method analysis is produced and analyzed in ANSYS 2020 R1. The plate featuring various polygonal shapes is meshed with over 396,000 solid elements and encompasses more than 1,716,880 nodes, all meeting acceptable criteria. A mapped meshing technique utilizing quadratic elements (for higher precision) has been employed to mesh the area surrounding the polygonal holes. The model of geometry is divided into small elements. The element has the capabilities having properties like plasticity, creep, stress stiffening, large deflections etc. The lower end of the plate is fixed in the model, while a compressive load is applied to its upper end. Finite element analysis was conducted on the polygonal hole shape within a finite plate under compression loading, with the subsequent calculation of equivalent (von Mises) stresses.

2.2 DOE RSM (Response Surface Methodology)

RSM, or Response Surface Methodology, comprises a collection of statistical and mathematical techniques used to develop empirical models. Its objective is to optimize an output variable, also

known as a response, influenced by several independent variables, or input variables, through careful experimental design. A set of quantitative experimental variables or factors and a response are examined in connection to each other using the Response Surface Method.

The number of sides, orientations of polygonal hole, areas of the polygonal hole, and applied load on a finite plate are four parameters taken into account in the calculation. A series of analyses is performed together the datasets for the RSM model.

The central composite design is utilized to determine the levels of control factors (number of sides of the polygonal hole, orientation, area of the polygonal hole, and applied load to the plate) in order to achieve an optimal response value, namely the stress concentration factor. A standard process of RSM method gives the regression response equation in uncoded units is as follows.

Response = 5.6124 - 0.2361 Polygon Hole + 0.2711 Orientation + 0.5817 Hole Area
+ 0.0428 Applied Load - 0.474 Polygon Hole*Polygon Hole
+ 0.171 Orientation*Orientation + 0.116 Hole Area*Hole Area
+ 0.146 Applied Load*Applied Load - 0.3731 Polygon Hole*Orientation
+ 0.0294 Polygon Hole*Hole Area + 0.0469 Polygon Hole*Applied Load
+ 0.1556 Orientation*Hole Area + 0.0481 Orientation*Applied Load

The results acquired through FEA methods are utilized to derive the response equation via the RSM approach.

The utilization of FEM-based response surface methods has significantly reduced the time and effort needed to assess the design variables of implants. With the hybrid model RSM and FEA, total twenty-five number of experiments are given by RSM method. These experiments are carried out to reduce material and time. These twenty-five numbers experiments are compared with RSM and FEA results.

3. Experimental Work

In this experimental study, the plate is assumed to be finite, isotropic, and linearly elastic. A finite plate implies that one side of the polygonal hole should be parallel to the x-axis.

3.1 Experimental Setup

Figure 3: *Photo elasticity experimental apparatus*

In this study, a photoelastic circular polariscope is utilized to determine the maximum stresses in isotropic finite plates featuring central polygonal holes of various configurations. Figure 3 depicts an image of the photoelastic apparatus used for experimental purposes. This setup was constructed with assistance from Aeolus Aerotech Pvt. Ltd, Bangalore. The purpose

of this experimental unit is to illustrate how materials behave in relation to external forces. Using the photoelasticity theory, specimens can be subjected to forces and/or stresses to observe the stress pattern and calculate the stress concentration factor. Figure 4 shows images of the polycarbonate plate holding on a photoelastic apparatus and a circular plate under compression loading for calibration process.

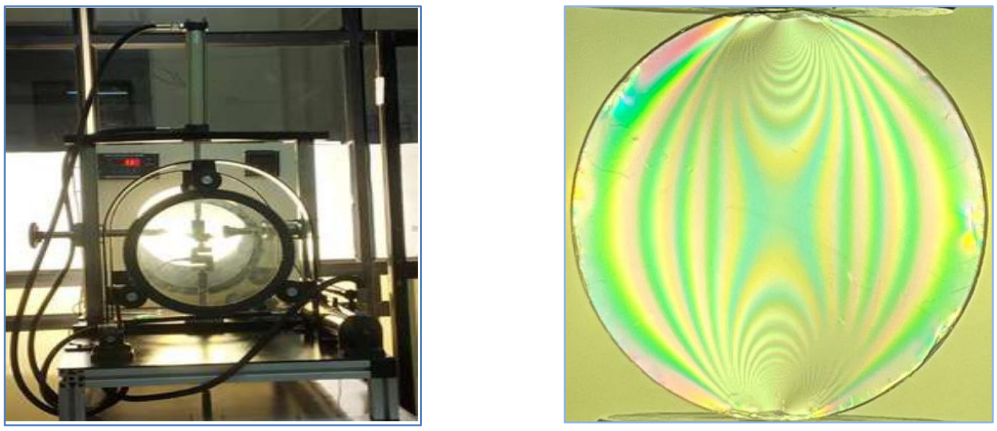

(a) photoelastic apparatus *(b) calibration*

Figure 4: *Images of the polycarbonate plate having square hole under compression loading and circular disk under compression for calibration process*

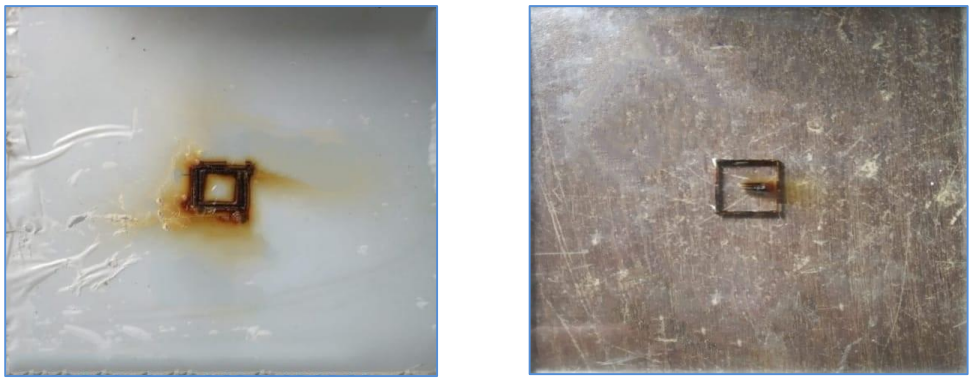

(a) Sample plate 1 *(b) Sample plate 2*

Figure 5: *Polycarbonate plate after laser machining*

This photo elasticity unit consists of:

- Analyzer and polarizer,
- Two quarter wave plate,
- Monochromatic and white light source,
- Rotatable analyzer with angular measurements,
- Mechanical load frame with a load capacity of 1.2 kN equipped with a digital load indicator for both tension and compression measurements.

3.2 Material Selection for Experimental Work

In the present work, a polycarbonate (PC) plate is used as workpiece material. It is photoelastic material and widely used for photoelasticity experiments as it demonstrates a birefringent property

essential for conducting photoelastic experiments. In industries variety of polycarbonates are available. This polycarbonate plate is photoelastic material and it exhibits a birefringence property which is needed for any photoelastic experiments. A few samples of acrylic plates are tested to check the results in the form of fringes and tried to minimize the cost of the workpiece as polycarbonate materials are very expensive. But experimentation on acrylic material shows the poor quality of fringes under axial compression loading conditions. So here all experimentations were carried out on a polycarbonate material. Figure 5 (a) and (b) show the specimens made from polycarbonate plates after laser machining. As we can see in the figures, laser cutting in a polycarbonate material is not possible due to the burning of the material as start the machining on polycarbonate with laser cutting. Here, polycarbonate is cut in to necessary shape of polygon shape holes by CNC water jet cutting machine. 16 specimens of 100 × 100 × 5 mm specimens are cut from each sheet for photo elastic experiment subjected to axial compression loading. Figure 6 shows the geometry of the plate having triangular, square, pentagonal and hexagonal holes after water jet machining.

3.3 Calibration of a Material

As shown in Figure 4(b), a standard calibration specimen is the circular disk used in diametral compression. The fringe constant value for selected material can be experimentally determined by the standard calibration procedure for materials. The value of the fringe constant f_σ can be determined experimentally by a model that is made of the same material as the specimen, by observing the corresponding value of N. For this specimen, the diameter D was 63.50 mm, and the load was 1.4 kN. The value of N at the center of the disk, as seen in Figure 4(b), is about 5.0. By following this procedure, we determined that the fringe constant for the selected material is approximately 11 kN/m/fringe [16].

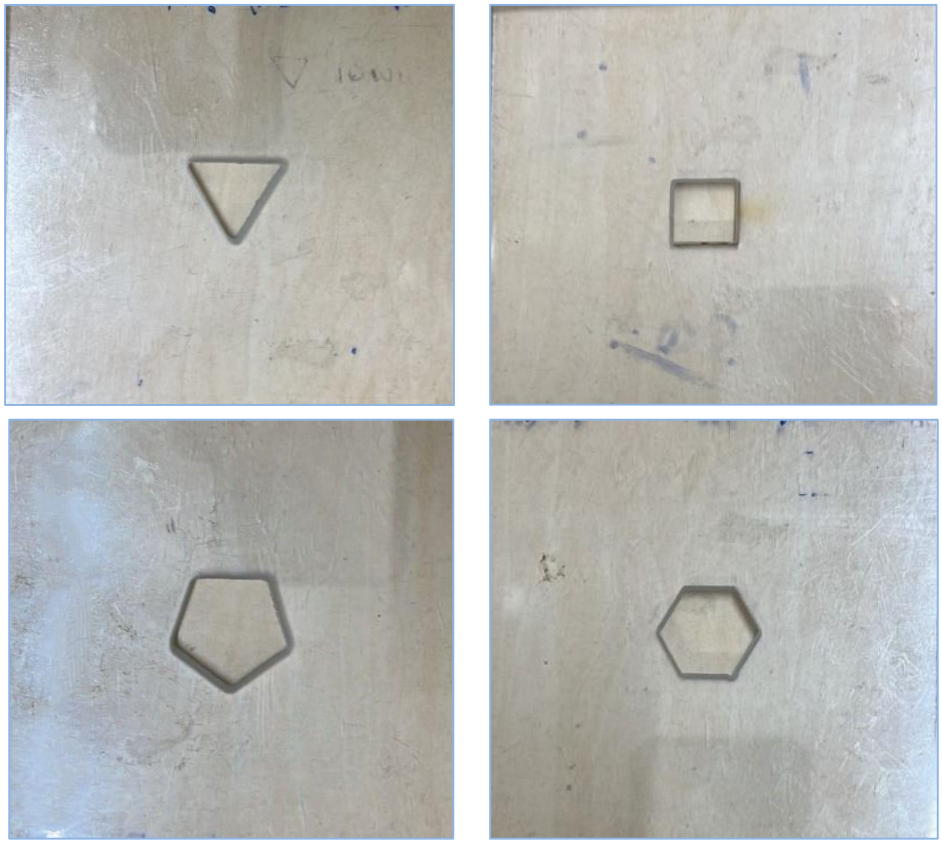

Figure 6: *Polycarbonate plate with various polygonal hole after water jet machining*

3.4 Experimental Procedure and Evaluation Method of SCF

For experiment work, the test specimen is to be held in different positions for different parameters. Figure 4 shows the photoelastic apparatus and the test specimen position for axial compression loading. Total of twenty-five experiments with various polygonal hole side, orientation (hole), constant areas (hole), and applied loads on a plate are performed under axial compression loading. Figure 8 to 10 shows the images captured during photo elastic experimental work for a various parameter. For optimum condition twenty fine experiments of different parameters are performed.

A stress concentration factor is a ratio of the maximum (highest) stress in the element to the nominal (reference) stress.

$$K_t = \frac{\sigma_{max}}{\sigma_{nom}} \tag{3}$$

$$\sigma_{nom} = \frac{P}{(H-\mathrm{d}) \times t} \tag{4}$$

Where, σ_{max} =The maximum stress at the corner of the polygonal hole on the plate occurs in the test specimen during experiments and is determined using a formula derived from the stress optic law theory for the Photoelasticity method.

$$\sigma_1 - \sigma_2 = \sigma_{max} = \frac{Nf_\sigma}{t} \tag{5}$$

σ_2 is zero considered as uniaxial directional loading [7].

$\sigma_{nom} = \frac{P}{(H-\mathrm{d}) \times t}$ for thick plate under axial compression

N = Fringe order

f_σ = The material fringe value is expressed in kN/m and is dependent on the wavelength of the light.

t = Thickness of the plate in mm

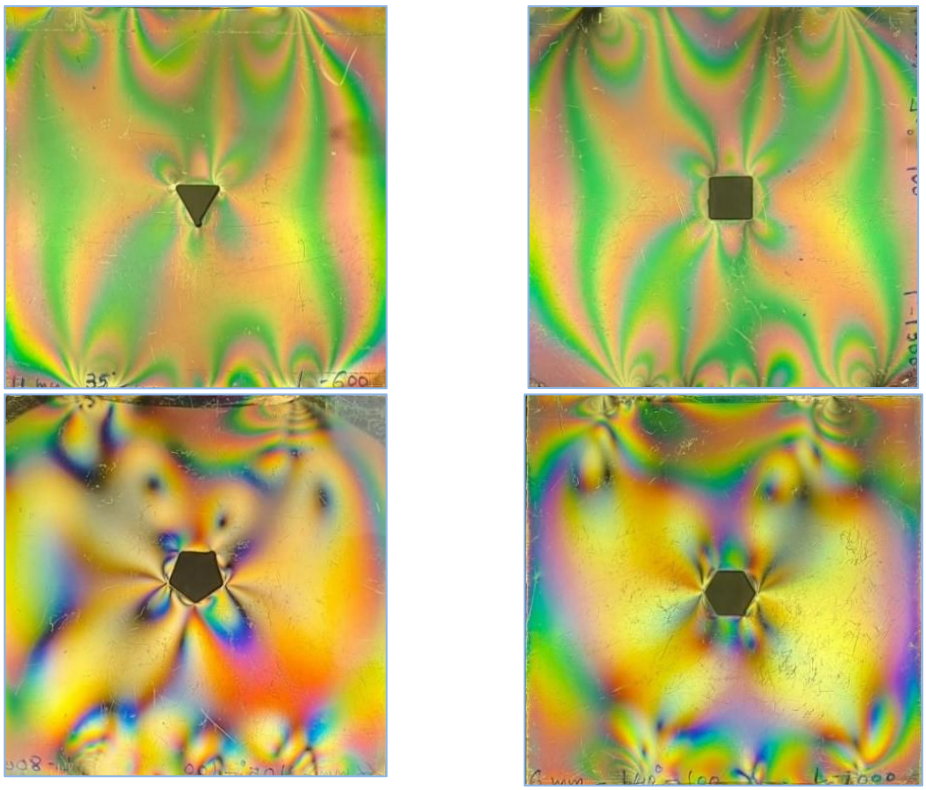

Figure 7: *Fringes generation in a plate with various polygonal holes at 0° orientation*

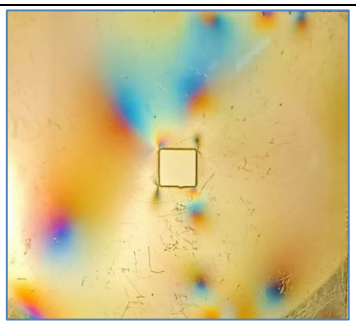

(a) n4 O70 A100 P600

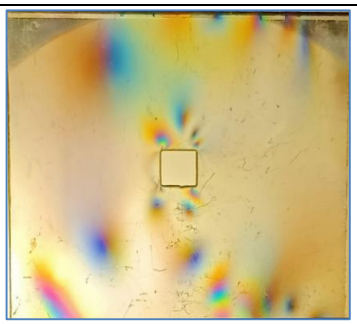

(b) n4 O70 A100 P1000

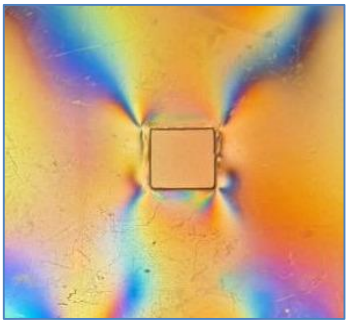

(c) n4 O70 A300 P600

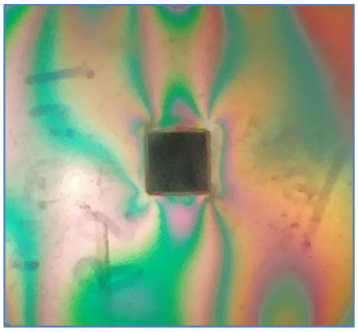

(d) n4 O70 A300 P1000

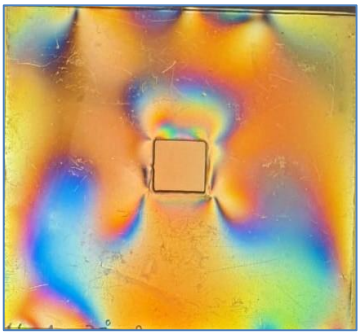

(e) n4 O105 A200 P800

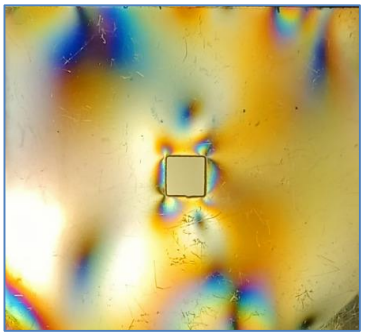

(f) n4 O140 A100 P600

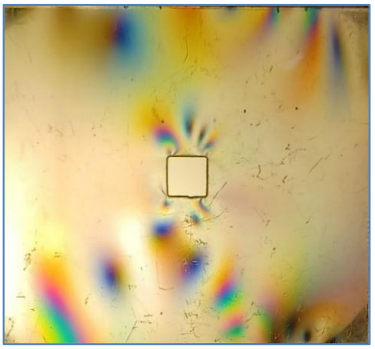

(g) n4 O140 A100 P1000

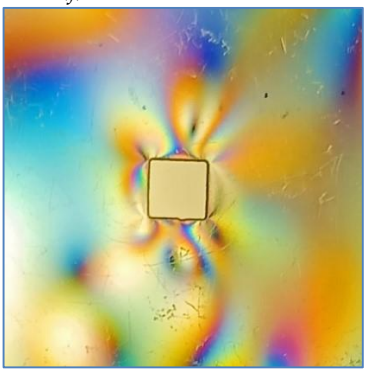

(h) n4 O140 A300 P600

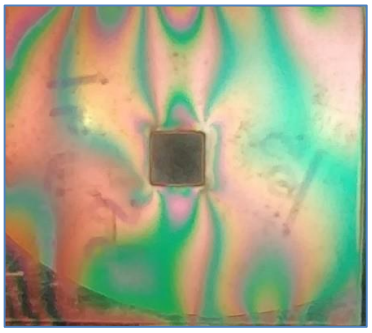

(i) n4 40 A300 P1000

Figure 8: *Images of specimen sample captured during photoelastic experimental work (n = 4)*

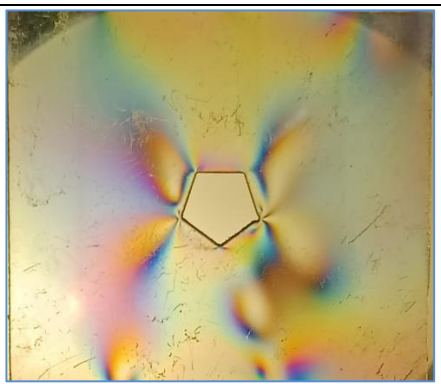

(j) n5 O70 A200 P800

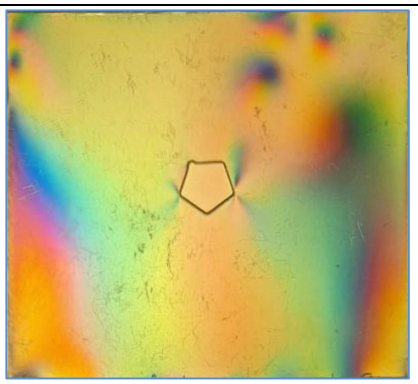

(k) n5 O105 A100 P800

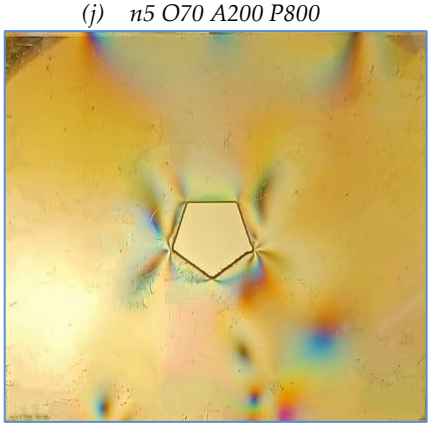

(l) n5 O105 A200 P600

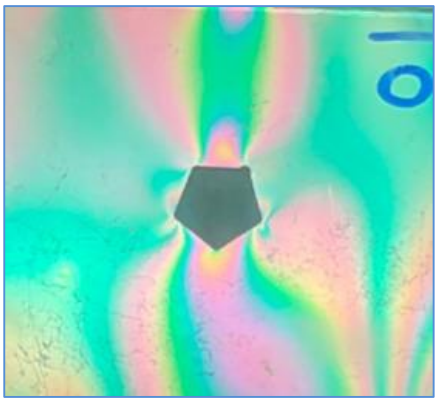

(m) n5 O105 A200 P800

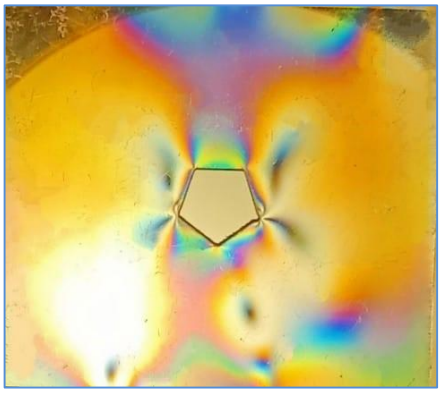

(n) n5 O105 A200 P1000

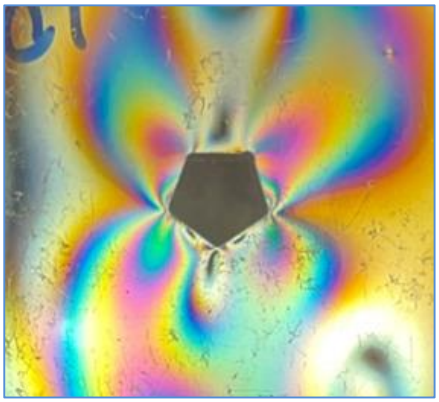

(o) n5 O105 A300 P800

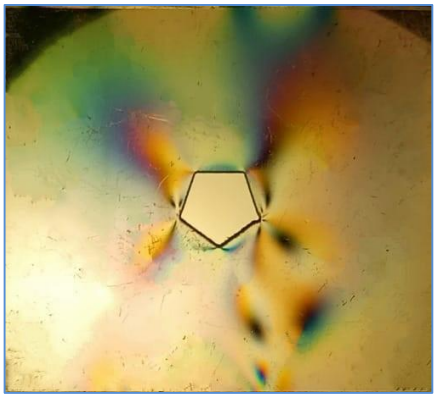

(p) n5 O140 A200 P800

Figure 9: *Images of test specimen captured during photoelastic experimental work (n = 5)*

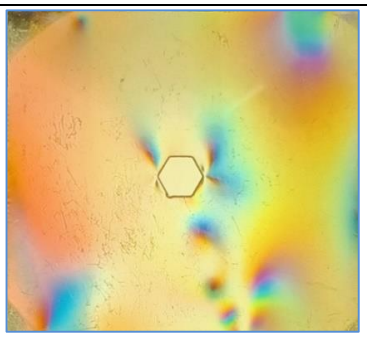

(q) n6 O70 A100 P600

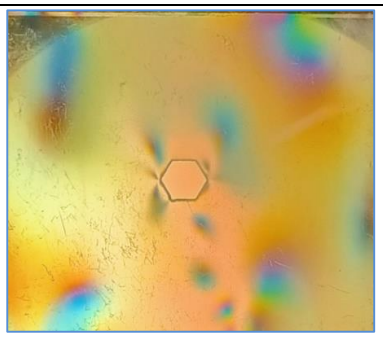

(r) n6 O70 A100 P1000

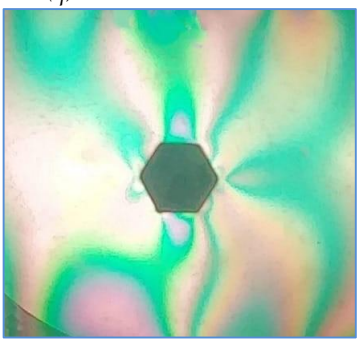

(s) n6 O70 A300 P600

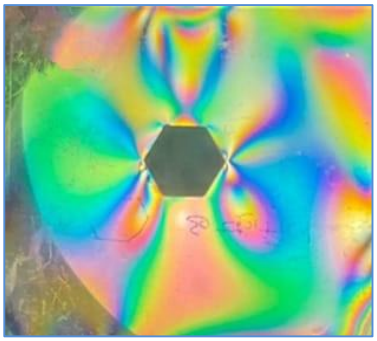

(t) n6 O70 A300 P1000

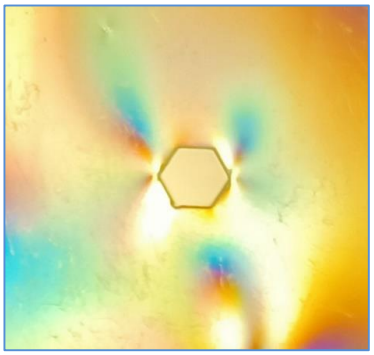

(u) n6 O105 A200 P800

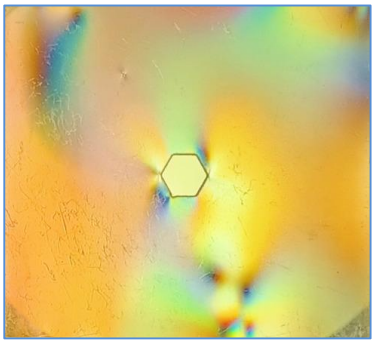

(v) n6 O140 A100 P600

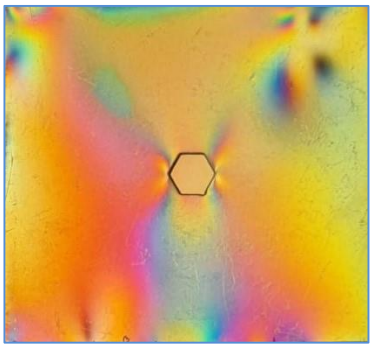

(w) n6 O140 A100 P1000

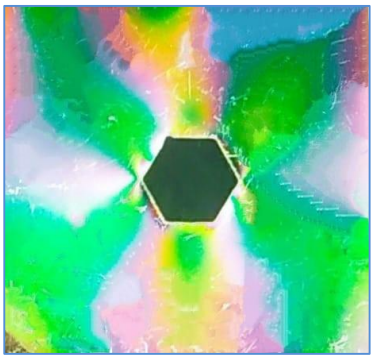

(x) n6 O140 A300 P600

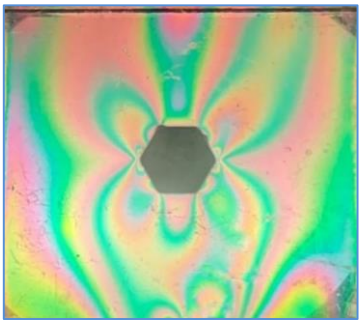

(y) n6 O140 A300 P1000

Figure 10: *Images of test specimen captured during photoelastic experimental work (n = 6)*

Before the starting of twenty-five experiments given by the DOE (RSM) methods, here are some results presented for the triangular, square, pentagonal and hexagonal holes at orientation angle 0°, hole area 100 mm² and applied load on the plate is 1000N.

For the parametric study, various plate parameters are taken into account, while ensuring that one edge of each polygonal hole remains parallel to the x-axis, with a fiber orientation of 0° (initial position of the plate). The selected load value is determined based on the feasible load range applied through the experimental setup, and the same load range is applied during the experiments. The experimental results in terms of fringes for various parameters combinations given by the RSM method are presented in Figure 8 to 10.

Here, in Figure 8 to 10, n represents the number of sides of the polygonal hole in a plate, O represents polygonal hole orientation (°), A represents the area of the polygonal hole (mm²) and P represents an applied load (N).

Table 1: *Results of photoelastic experimental work of finite plate*

L (mm)	H (mm)	t (mm)	n	O (°)	A (mm²)	P (N)	N	f_σ kN/m	Max. stress (N/mm^2)	Nominal stress (N/mm^2)	SCF
100	100	5	4	70	100	600	3	11	6.6	1.38	4.80
100	100	5	4	70	100	1000	5	11	11.0	2.29	4.80
100	100	5	4	70	300	600	4	11	8.8	1.54	5.71
100	100	5	4	70	300	1000	6.6	11	14.5	2.57	5.65
100	100	5	4	105	200	800	4.13	11	9.1	1.94	4.70
100	100	5	4	140	100	600	4	11	8.8	1.40	6.30
100	100	5	4	140	100	1000	6.1	11	13.4	2.33	5.76
100	100	5	4	140	300	600	5.13	11	11.3	1.59	7.10
100	100	5	4	140	300	1000	8.6	11	18.9	2.65	7.15
100	100	5	5	70	200	800	5	11	11.0	1.92	5.72
100	100	5	5	105	100	800	4	11	8.8	1.82	4.85
100	100	5	5	105	200	600	3.6	11	7.9	1.44	5.49
100	100	5	5	105	200	800	4.6	11	10.1	1.92	5.26
100	100	5	5	105	200	1000	6	11	13.2	2.41	5.49
100	100	5	5	105	300	800	6	11	13.2	2.02	6.55
100	100	5	5	140	200	800	5	11	11.0	1.93	5.71
100	100	5	6	70	100	600	3.1	11	6.8	1.36	5.02
100	100	5	6	70	100	1000	5.13	11	11.3	2.26	4.98
100	100	5	6	70	300	600	4	11	8.8	1.50	5.85
100	100	5	6	70	300	1000	6.6	11	14.5	2.51	5.79
100	100	5	6	105	200	800	4.6	11	10.1	1.93	5.25
100	100	5	6	140	100	600	3	11	6.6	1.37	4.83
100	100	5	6	140	100	1000	4.6	11	10.1	2.28	4.44
100	100	5	6	140	300	600	4	11	8.8	1.52	5.78
100	100	5	6	140	300	1000	7.6	11	16.7	2.54	6.59

Table 1 shows the results of photoelastic experimental work on 5 mm thick plates under axial compression loading. Also, Table 1 presents twenty-five experimental results for various polygonal hole sides, orientations (holes), constant hole areas, and applied loads. Based on the obtained results, the maximum stresses of the polygonal holes within the finite flat plates are identified and utilized for calculating the stress concentration factor.

4. Results and Discussion

There are no methods available for choosing a polygonal hole in a plate that will provide the lowest SCF for a particular geometry following the industry standard for hole design in plates. Therefore, efforts are being made to develop criteria for the selection of a polygonal hole in a plate that will give the least SCF. The FEA, design of experiment (RSM), and experimental method as photoelasticity, are presented in the previous section.

A range of SCF is developed for triangular, square, pentagonal, and hexagonal holes under uniaxial compression loading. Optimal polygonal hole shapes, orientations, areas, and applied loads on the plate are determined from various ranges of SCF. Here, results obtained from the DOE (RSM) and FEA methods are compared with those from photoelasticity experimental methods.

It is observed from Figure 8 to 10 that the vertices are points of high stress concentration in a plate. Hence, the stress field in a finite isotropic plate can be influenced by factors such as the number of vertices, their positions, and the direction of loading along a specific axis.

Table 2: *SCF obtained for various polygonal shape hole in a plate from FEA, RSM and Photoelasticity.*

L (mm)	H (mm)	t (mm)	n	O (°)	A (mm^2)	P (N)	FEA SCF	RSM SCF	Experimental SCF	(%) Error FEA vs Experiment	(%) Error RSM vs Experiment
100	100	5	4	70	100	600	4.72	4.95	4.80	-1.6	3.10
100	100	5	4	70	100	1000	4.72	4.95	4.80	-1.6	3.13
100	100	5	4	70	300	600	5.69	5.99	5.71	-0.3	4.74
100	100	5	4	70	300	1000	5.69	5.98	5.65	0.7	5.60
100	100	5	4	105	200	800	4.94	5.00	4.70	4.9	6.09
100	100	5	4	140	100	600	5.9	6.17	6.30	-6.8	-2.02
100	100	5	4	140	100	1000	5.9	6.17	5.76	2.3	6.51
100	100	5	4	140	300	600	7.14	7.49	7.10	0.5	5.22
100	100	5	4	140	300	1000	7.15	7.30	7.15	0	2.05
100	100	5	5	70	200	800	5.55	5.51	5.72	-3.1	-3.83
100	100	5	5	105	100	800	5.08	4.80	4.85	4.6	-0.95
100	100	5	5	105	200	600	5.68	5.72	5.49	3.4	3.97
100	100	5	5	105	200	800	5.68	5.61	5.26	7.4	6.28
100	100	5	5	105	200	1000	5.68	5.60	5.49	3.4	1.99
100	100	5	5	105	300	800	6.22	6.31	6.55	-5.3	-3.76
100	100	5	5	140	200	800	5.86	6.05	5.71	2.5	5.67
100	100	5	6	70	100	600	5.02	5.35	5.02	0	6.13
100	100	5	6	70	100	1000	5.02	5.35	4.98	0.7	6.82
100	100	5	6	70	300	600	5.76	6.15	5.85	-1.6	4.86
100	100	5	6	70	300	1000	5.76	5.85	5.79	-0.6	0.96
100	100	5	6	105	200	800	5.18	5.33	5.25	-1.4	1.45
100	100	5	6	140	100	600	4.36	4.60	4.83	-10.7	-4.96
100	100	5	6	140	100	1000	4.36	4.60	4.44	-1.9	3.42
100	100	5	6	140	300	600	5.69	5.95	5.78	-1.6	2.83
100	100	5	6	140	300	1000	6.45	6.61	6.59	-2.2	0.33

In Table 2, twenty-five results each for FEA, RSM, and photoelasticity are tabulated for various polygonal hole shapes, orientations, constant hole areas, and applied loads on a plate. The maximum

stresses of the plates with holes are determined from the study and employed in the calculation of the stress concentration factor (SCF).

Table 2 show the comparison of SCFs based on FEA, RSM, and photoelasticity experiments for different polygonal hole shapes (N = 4, 5, 6), orientation angles (70°, 105°, 140°), polygonal hole areas (100, 200, 300), and applied loads (600 N, 800 N, 1000 N). Observations from Table 2 indicate, that as the size of the polygonal hole increases, the stress concentration also increases. Figure 8 to 10 shows that the generated stress concentration factor varies at various orientations of the polygonal holes due to its rotation concerning the loading direction.

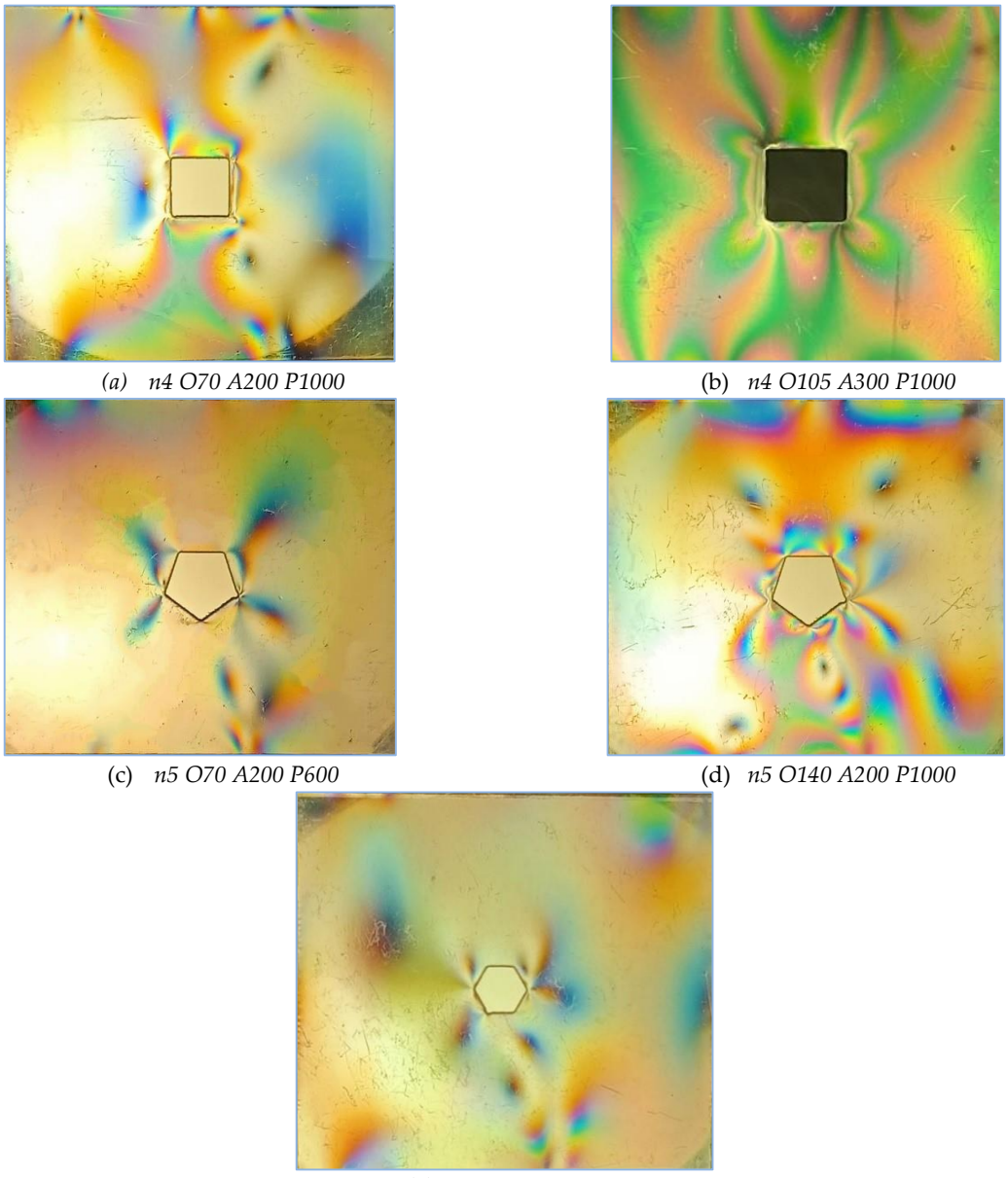

(a) n4 O70 A200 P1000

(b) *n4 O105 A300 P1000*

(c) *n5 O70 A200 P600*

(d) *n5 O140 A200 P1000*

(e) *n6 O105 A100 P800*

Figure 11: *Images of test sample captured during photoelastic experimental work (intermediate)*

Intermediate results from experiments and finite element analysis are essential for validating the outcomes of various methods. The validation of the obtained RSM equation is carried out by performing experiments and FEA for the intermediate readings (these readings not covered in Table 2) and presented in Table 3 and, the experiment results for various parameter combinations (these readings not covered in Table 2), are presented in Figure 11.

Table 3: *SCF obtained for various polygonal shape hole in a plate from FEA, RSM and Photoelasticity (validation results).*

L (mm)	H (mm)	t (mm)	n	O (°)	A (mm²)	P (N)	FEA SCF	RSM SCF	Experimental SCF	Error FEA vs Experiment (%)	Error RSM vs Experiment (%)
100	100	5	4	70	200	1000	5.33	5.50	5.40	-1.4	1.76
100	100	5	4	105	300	1000	5.24	5.35	5.20	0.7	2.79
100	100	5	5	70	200	600	5.55	5.60	5.49	1.0	1.92
100	100	5	5	140	200	1000	5.86	6.00	6.03	-2.9	0.50
100	100	5	6	105	100	800	4.36	4.60	4.34	0.4	5.55

Among this all parameters, when we are considering three parameters as a constant, and variable as a one parameter, it is shows results as presented in the Figure 12.

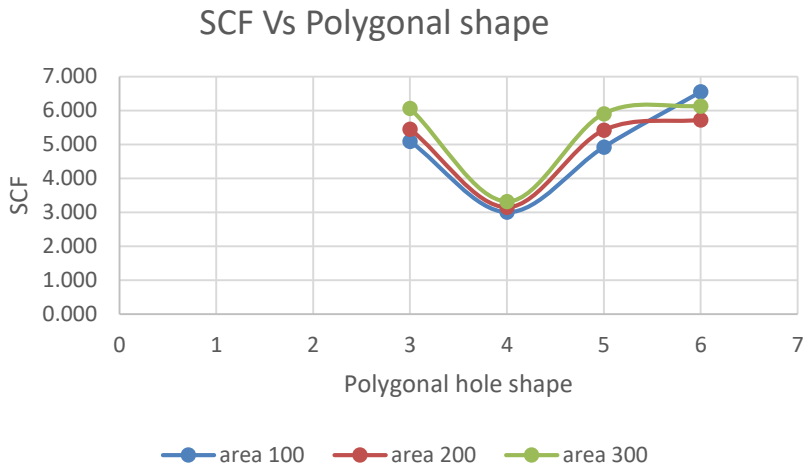

Figure 12: *SCF vs. polygonal hole shape*

4.1 Effect of Polygonal Hole Shape on a Finite Plate

For uniaxial Y loading, the maximum values of SCF are observed for the center positions of holes in the case of n = 3 and n = 5, while the minimum values of SCF are observed for the center positions of holes with n = 4 and n = 6. This may be because triangular and pentagonal holes have two vertices on the X-axis (at 0°), while the rest of the vertices lie in the plane. On the other hand, square and hexagonal holes have one vertex on the X-axis (at 0° and 180°) and the others lie in the plane. It is noted that the locations of high stress concentration are similar in both square (n = 4) and hexagon (n = 6) shapes, as both exhibit symmetry concerning to the X-Y axis. Figure 12 shows a graph of SCF versus polygonal hole shape. It is observed that increasing the number of sides of a polygon affects the observed minimum and maximum values of SCF generation. For example, square and hexagonal holes are symmetrical about the x and y axes, resulting a range of SCF is between 3.01 to 6.16 and 4.01 to 6 respectively. Therefore, the difference between the maximum and minimum values of SCF is larger. Conversely, triangular and pentagonal holes, which are non-symmetrical about both the x and y axes, generate higher SCF values but with a range of SCF is between 4.26 to 4.94 and 5.36 to 6.01 respectively. Consequently, the difference between the maximum and minimum values of SCF is smaller. For unidirectional and static loading, it is advised to use square and hexagonal holes oriented in such a way that generate SCF value 3. The recommendation is to employ triangular and pentagonal holes arranged in a manner that produces minimal variations in SCF, ranging between 4 to 6. These triangular and pentagonal shapes of polygonal holes generate higher SCF, but they can

sustain variable loads. The direction of loading determines the appropriate orientation of polygonal holes during the design of the structure.

4.2 Effect of Orientation of Polygonal Hole

For uniaxial Y loading, if the maximum vertices (corners) are along the X-axis, it shows the highest stresses in all the polygonal holes. The vertex of the highest stress is not necessarily on the X or Y axis but may lie in a plane depending on the geometry of the polygonal shape. As a special case, for square holes with 0°, 90°, and 180° angles, the minimum SCF is obtained. Due to the maximum distance generated between two corners of the square hole when positioned parallel to the loading direction, the maximum SCF shall be at 45° and 135° angles, indicating parallel edges of the square holes in the direction of loading, thereby always reducing the stresses by up to 50%. As we maintain the variable as the orientation of the polygonal hole, while considering other parameters as constant, increasing the orientation of the hole for selected parameters results in an increase in the SCF value up to a certain orientation. After reaching this point, further increases in orientation lead to a decrease in the SCF value.

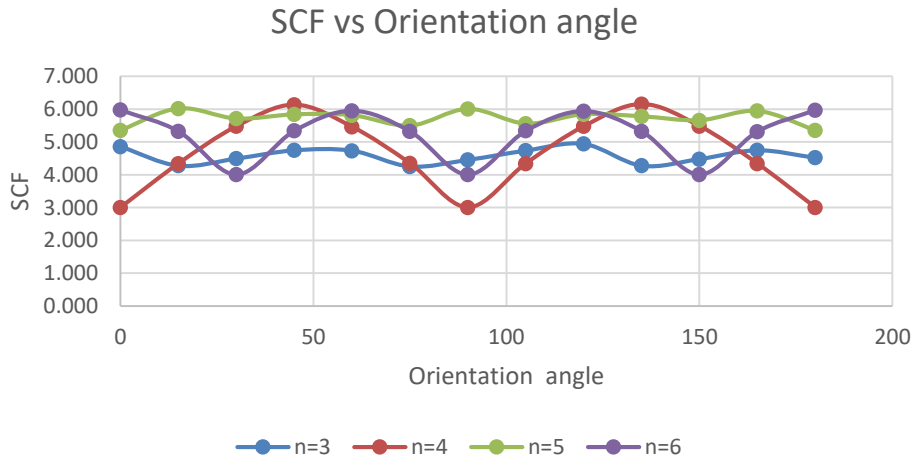

Figure 13: *SCF vs. Orientation angle*

It has been observed that the curve exhibits a repeating nature at certain orientations. Specifically, the curve repeats at intervals of 60°, 90°, 75°, and 60° for triangular, square, pentagonal, and hexagonal shapes respectively. This phenomenon arises due to the geometry of the hole's shape. Figure 13 illustrates a graph of SCF versus the orientation of the polygonal hole shape.

4.3 Effect of the Area of Polygonal Hole

As far as the area of the polygonal hole is concerned, if the area of any polygonal hole increases in a finite plate, the net area will always reduce, generating more stresses and a higher Stress Concentration Factor (SCF). The SCF of all shapes is found to increase as the number of polygon sides increases for a constant area. It is observed that hole and symmetry are more affected by SCF for the same area of all shapes of the polygonal hole. As we keep the variable as the area of the polygonal hole and other parameters constant, an increase in the area of the polygonal hole in a finite plate always results in a reduction in the net area, thereby increasing the stresses and SCF. Figure 14 shows a graph of SCF vs. the constant area of the polygonal hole shape.

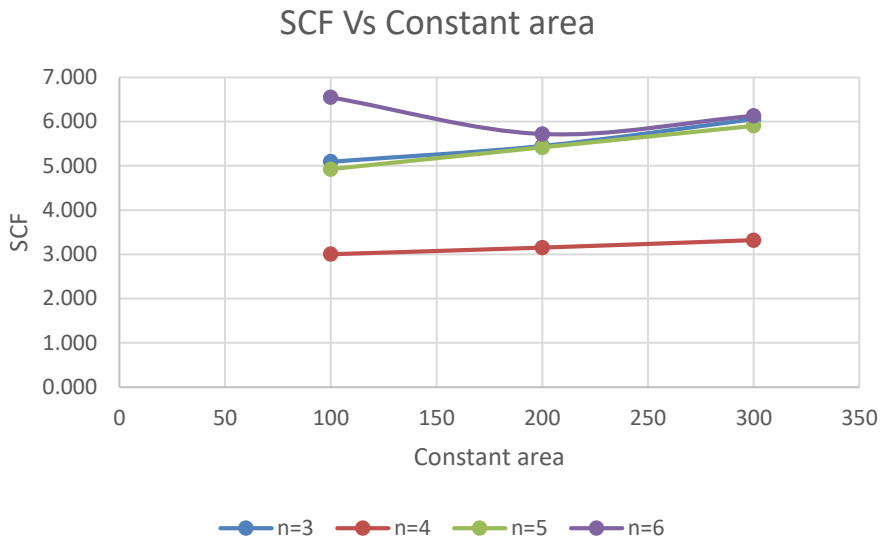

Figure 14: *SCF vs. Constant area of polygonal hole*

4.4 Effect of Applied Load on a Finite Plate

If the applied load on the finite plate is increasing, it does not produce any significant effect on the stress concentration factor for all polygonal shapes in a finite plate. As the load increases on the plate, von Mises stresses increase, and simultaneously nominal stresses also increase, showing a negligible effect on the SCF. Therefore, the applied load is not a significant factor for the SCF for the presented load cases and load range (600 N to 1000 N).

5. Conclusion

A numerical verification of the presented method is carried out using the ANSYS software, Minitab, and a good agreement of stress distributions is found.

It is advised to use square and hexagonal shaped holes at particular orientations when minimum stress concentration factor values are generated is 3.00 for unidirectional and static loading. At points where there is no or negligible variation in load occurs it's advisable to use triangular and pentagonal holes at suitable orientations, where the stress concentration factors generate within the range of 4.00 to 6.00. During the design stage, the direction of loading and arrangement of the orientation of these polygonal shapes are important factors to study.

Among all holes, when the baseline is parallel to the x-axis, the increasing order of stresses and SCF is as follows: square, triangular, pentagonal, and hexagonal.

The stress concentration factor is significantly influenced when one of the corners of the polygonal hole aligns with the loading direction. Consequently, as the side ratio increases, a square hole exhibits the minimum SCF compared to triangular, pentagonal, and hexagonal holes.

A square-shaped hole yields a 40% lower minimum stress concentration factor compared to a hexagonal-shaped hole, primarily because a greater number of edges are parallel to the loading directions

It is preferable to create a hole with the maximum number of edges parallel to the loading direction.

The stress concentration factor rises with an increase in the side ratio for a specific polygonal hole shape, owing to the enlargement of the hole and its area. Larger holes with more edges result in a higher SCF value due to the presence of additional corners.

References

[1] M. Ismail, L. Žiković, N. Čeh, and G. Jelenić. (2022). Experimental and numerical analysis of stress concentration in a plate with a circular hole. *10th International Congress of Croatian Society of Mechanic, 10*:1-2.

[2] Manish Pandey, Aprajita Patel, Kshitiz Jaiswal, Lalit Kirola, and Subodh Kumar Sharma. (2021). Investigation of Variation in Stress Concentration Factor with the Change in Orientation of Central Hole on a Rectangular Plate. *Recent Advances in Mechanical Engineering, Lecture Notes in Mechanical Engineering, 77: 629-635.*

[3] X. Zhang, A. Lu, K. Song, G. Wu, and L. Wang. (2022). Methodology for Determining the Compliance Matrix and Analyzing the Skew Anisotropic Plate with an Arbitrarily Shaped Hole. *Advances in Materials Science and Engineering. 2022:1–14, doi: 10.1155/2022/5949398.*

[4] YI, W., RAO, Q. H., MA, W. B., SUN, D. L., and SHEN, Q. Q. (2020). A new analytical-numerical method for calculating interacting stresses of a multi-hole problem under both remote and arbitrary surface stresses, *Appl. Math. Mech. -Engl. Ed. 41:1539-1560, doi: https://doi.org/10.1007/s10483-020-2653-9.*

[5] W. Wang and B. J. Spencer. (2021). Numerical solution for the stress near a hole with corners in an infinite plate under biaxial loading. *Journal of Eng Math. 127:1-131, doi: 10.1007/s10665-021-10104-8.*

[6] S. Badiger and R. D. S. (2023). Stress distribution in an infinite plate with discontinuities like elliptical or circular hole by boundary force method, *SN Appl. Sci., 5:77, doi: 10.1007/s42452-023-05289-9.*

[7] B. Safaei, Z. Pezeshki, K. Kotrasova, and E. Kormanikova. (2022). Analysis of stress concentration at the edge of hole in plates with different widths by using FEM. *IOP Conf. Ser.: Mater. Sci. Eng. 1252:1-11, doi: 10.1088/1757-899X/1252/1/012067.*

[8] P. Jaiswal, S. Makin, A. D. Dubey, and G. Ghangas. (2022). Analysis of stress concentration reduction around rounded rectangular slot with FGM ring. *Materials Today: Proceedings, vol. 50:1953–1957, doi: https://doi.org/10.1016/j.matpr.2021.09.323.*

[9] P. Rani, D. Varma, and G. Ghangas. (2022). Stress concentration analysis of functionally graded material coated elliptical inclusion under uniaxial tension. *Materials Today: Proceedings, 78:351-358, doi: https://doi.org/10.1016/j.matpr.2022.09.602.*

[10] O. Maksymovych, T. Solyar, A. Sudakov, I. Nazar, and M. Polishchuk. (2021). Determination of stress concentration near the holes under dynamic loadings, *Nauk. visn. nat. hirn. Univ. 3:19–24., doi: 10.33271/nvngu/2021-3/019.*

[11] O. V. Maksymovych and T. Ya. Solyar. (2022). Determination of Stress Concentration Near Dies, Holes, and Cracks in the Half Plane Based on the Method of Integral Equations and Green Solutions. *Journal of Math Sci, 261:162–175, doi: 10.1007/s10958-022-05745-8.*

[12] M. Patil and Ajay More. (2021). Effect of Hexagonal Cutout Orientation and Roundness of Edges on Stress Concentration in Plate. *International Research Journal of Engineering and Technology (IRJET), 08:4431–4435.*

[13] M Mohan Kumar, Rajesh S, Yogesh H, and Yeshaswini B R. (2013). Study on the Effect of Stress Concentration on Cutout Orientation of Plates with Various Cutouts and Bluntness. *International Journal of Modern Engineering Research (IJMER), 3:1295–1303.*

[14] R. H. Patel and B. P. Patel. (2023). Analyzing Stress Concentration Factor in Finite Plate with Different Polygonal Discontinuities Under Uniaxial Compression Using FEM. *Journal of Kejuruteran. 35:1033–1043, doi: 10.17576/jkukm-2023-35(5)-05.*

[15] R. H. Patel and B. P. Patel. (2022). Effect of various discontinuities present in a plate on stress concentration: a review. *Engineering Research Express, 4:1–15. doi: https://doi.org/10.1088/2631-8695/ac8c1b.*

[16] "James W. Phillips "Photoelasticity, Experimental Stress Analysis, TAM 326."